Received December 14, 2019, accepted December 30, 2019, date of publication January 15, 2020, date of current version January 29, 2020.
Digital Object Identifier 10.1109/ACCESS.2020.2966873

Evaluation of Ka-Band Rain Attenuation for Satellite Communication in Tropical Regions Through a Measurement of Multiple Antenna Sizes

P. M. KALAIVAANAN[1], (Student Member, IEEE), ADUWATI SALI[1], (Senior Member, IEEE), RAJA SYAMSUL AZMIR RAJA ABDULLAH[1], (Senior Member, IEEE), SYAMSURI YAAKOB[1], (Senior Member, IEEE), MANDEEP JIT SINGH[2,3], (Senior Member, IEEE), AND ALI M. AL-SAEGH[4], (Member, IEEE)

[1]WiPNET Department of Computer and Communication Systems, Faculty of Engineering, Universiti Putra Malaysia (UPM), Serdang 43400, Malaysia
[2]Department of Electrical, Electronic and Systems Engineering, Universiti Kebangsaan Malaysia (UKM), Bangi 43600, Malaysia
[3]Space Science Centre (ANGKASA), Institute of Climate Change, Universiti Kebangsaan Malaysia, Bangi 43600, Malaysia
[4]Computer Engineering Techniques, Al-Ma'moon University College, Baghdad 100001, Iraq

Corresponding author: P. M. Kalaivaanan (gs52374@student.upm.edu.my)

ABSTRACT The Ka-band is modifying the mode of legacy communication towards versatile satellite-oriented systems with the beam-spot capability and a high-throughput architecture to provide twice the capability of classic Fixed Satellite Service (FSS) satellites, thus significantly reducing the cost per bit. Given this background, the contribution of precipitation rate and Ka-band downpour attenuation are expected to improve statistical models for effect prediction. The International Telecommunication Union (ITU) and local researchers are working tirelessly to determine the best prediction model for tropical climates. However, persistent and continuous efforts are required because currently available models do not perform well. The current prediction model for large datasets exhibits a certain deviation. Direct beacon measurement has been compared with an available prediction model that analyses rain effects in tropical regions. Theoretically, the size of the antenna and its gain influence the performance of the receiving signal. Size and availability are two factors which cause degradation and outage in the receiving signal. The majority of extant studies focus on a single antenna with a diameter lesser than 2.4m. Theoretically, antennas with a smaller diameter possess a smaller margin in comparison with antennas with larger diameters. This condition could affect the prediction model when the high attenuation causes a rapid outage in a small antenna and lead to the unavailability of measurement results. To study such effects and provide a good recommendation, the current work measures the beacon attenuation data at two locations, namely, Bukit Jalil (Kuala Lumpur) and Cyberjaya (Selangor). The locations are approximately 15 km apart and have antennas from 0.65m to 31.1m in sizes. Analyses using an available prediction model revealed that ITU-R P.618 provides the lowest RMS value of 14.37 with regards to rainfall rate on two selected samples in Malaysia. High-accuracy prediction can be achieved through the contribution of this study, and comparative data can be obtained for future research. This study is an encouraging step towards a highly comprehensive and accurate prediction of tropospheric impairments in Ka-band satellite communications in the tropical region.

INDEX TERMS ITU, rain attenuation, Ka-band satellite communication.

I. INTRODUCTION

Rain attenuation is a dominant impairment because it produces a significant amount of loss. This loss results in the degradation of satellite-to-ground links and thus influences the reliability and performance of satellite communication links [1]–[4]. Satellite signal strength is reduced under severe rain conditions. Moreover, signal strength tends to decay at a faster pace when being operated under Ka-band frequency [3]. The majority of studies on the Ka-band propagation model have focused on European satellites, a few works have examined prediction performance in Malaysia.

The associate editor coordinating the review of this manuscript and approving it for publication was Vittorio Camarchia.

The rain prediction model has been established and used in recent years to provide reliable planning in communication systems. An accurate prediction model for the line of sight of satellite links is essential in planning and designing high-capacity, point-to-point and point-to-multipoint radio communication systems for frequency bands above 10 GHz [1]. Spectrum crunch disrupts the local operator and causes it to move to high operating frequencies, such as the millimetre-wave (mmWave). Researchers are combining their efforts to obtain a solution to this issue.

The International Telecommunication Union Radiocommunication Sector (ITU-R) model is widely used by many researchers [6], [7] and provides an almost accurate prediction. However, tropical regions require further optimization of the available ITU-R P.618 model because changes in rain patterns are uncertain.

Past research has indicated that three models, namely, ITU-R P.618, Dissanayake Allnut Haidara (DAH) and modified ITU-R [1], [2], [5], perform well in tropical regions with high rainfall intensity [5]. Many studies have been conducted in Malaysia [5]–[8], but the continuous effort is still required due to constant changes in the global climate. This situation is primarily due to global warming, which causes worldwide rainfall patterns to shift [9]. Communication systems are subjected to numerous fade occurrences under heavy rain.

The DAH and ITU-R attenuation models are similar, except for the parameter of rain height. The rain height is fixed at 5 km in the DAH model. Rain height for an area with a given latitude and longitude depends on mean annual zero degrees isotherm height as indicated in equation (1) [10].

$$hr = ho + 0.36 \text{ km} \tag{1}$$

hr = mean annual rain height above the mean sea level.
ho = mean annual 0 °C isotherm height above the mean sea level provided in an ITU R-REC-P.839-4 digital map.

The precipitation characteristics in tropical regions differ even though most of the recommended models are based on data obtained from temperate regions. This study aims to enhance prediction performance in a tropical region.

II. SYSTEM DESCRIPTION

The Ka-band propagation measurement system uses small to large antennas, as outlined in Figure 1. The aim is to ensure that no missing data exist and that all data are analysed precisely. The downlink receiving signal is passed on to the Carrier Monitoring System (CMS), where the component is placed in the same network. Village Island Village Flow RF monitoring (VF-SMON) is connected to ensure that the L-band signal is continuously logged parallel to the signal from all other receiving antenna.

A detailed propagation measurement setup is shown in Figure 2 to provide a clear understanding of the return downlink signal setup. The front end of the signal is shared with the digital tracking receiver (DTR) to measure the receiving beacon signal and integrate it into CMS. Most available systems such as in [12] uses the polling method with a round-robin mechanism when a parallel receiving system design is infeasible due to system limitations. This data logging mechanism

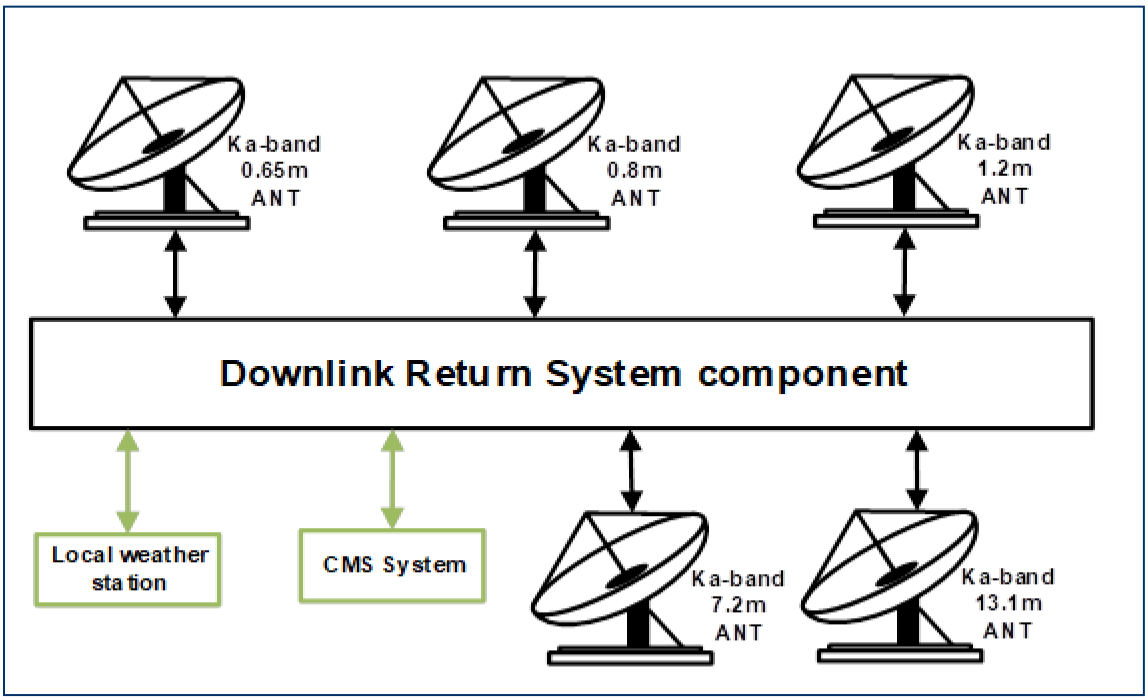

FIGURE 1. Typical block diagram of the system.

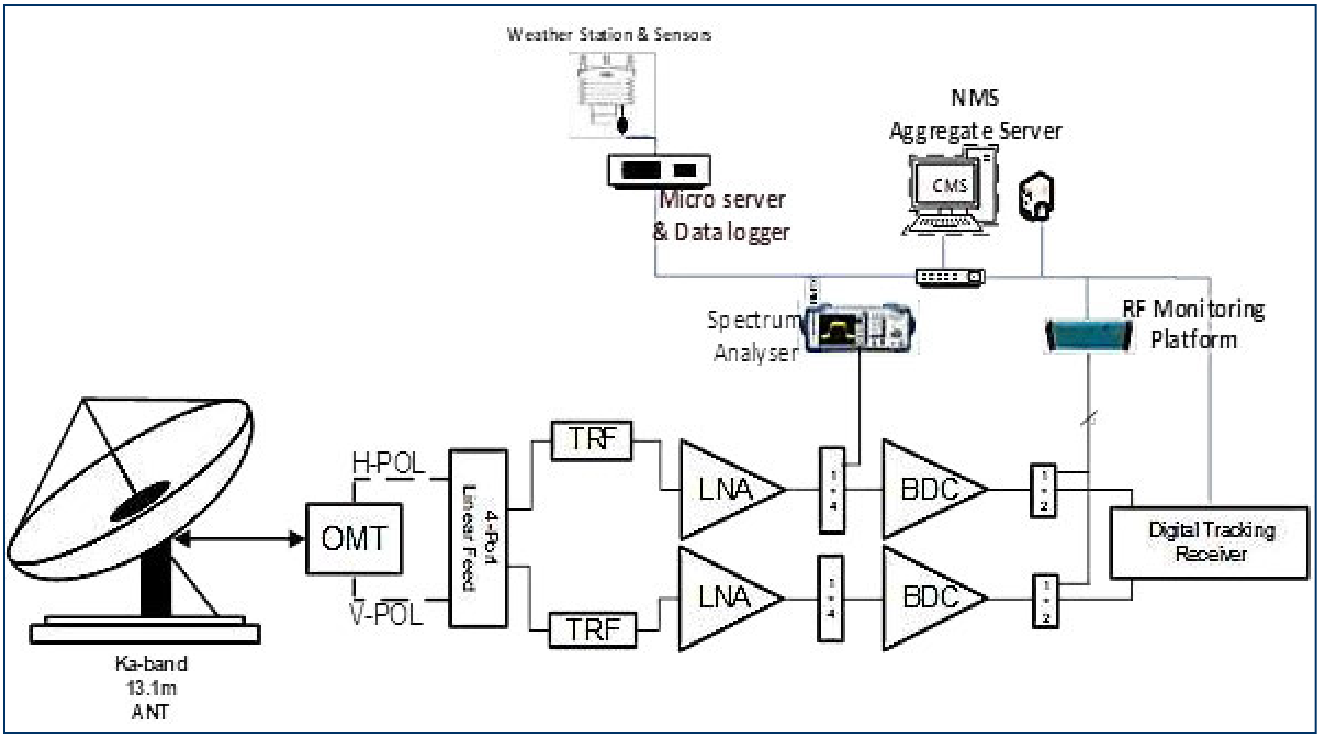

FIGURE 2. Ka-Band return downlink and weather station logging setup.

TABLE 1. Characteristics of downlink Ka-band systems.

Component/ Subsystem	Characteristics
Orthomode transducer (OMT)	Orthomode transducers serve either to combine or to separate two orthogonally polarized microwave signal paths.
TxRx Reject Filter (TRF)	Receive Bandpass filters are designed to offer rejection not only in the transmit frequencies but also above and below the receive band.
Low Noise Amplifier (LNA)	Is an electronic amplifier that amplifies the signal without significantly degrading its signal-to-noise ratio.
Block Down Converter (BDC)	Convert the receiving Ka-band signal to desire L-band.
Digital Tracking Receiver (DTR)	The DTR converts received satellite beacon signals to a DC voltage.
Network Monitoring System (NMS)	Proprietary virtual machine system that continually monitors and log the captured data.

could reduce the accuracy of the measured data. The design approaches can be utilized to recommend a good solution for ensuring that all data are obtained without missing.

Moreover, the data logger from the local weather station is incorporated into CMS to provide continuous data logging (mainly rain intensity and temperature) from onsite meteorological sensors, as shown in Figure 3.

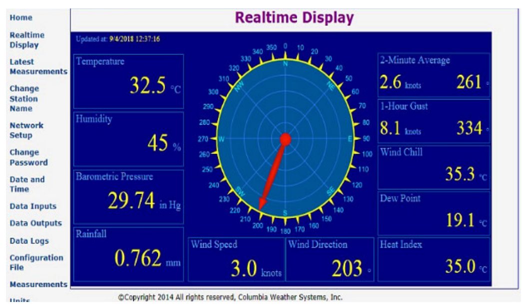

FIGURE 3. Display of real-time weather data.

Received Ka-band beacon signals are continuously measured with a spectrum analyzer (SA), which is fed from a 1:4 divider after the low-noise amplifier (LNA). The general-purpose interface bus (GPIB) connection from SA is integrated to transfer data to the CMS system for monitoring satellite uplink and downlink performance.

Consequently, real-time beacon signals (Figure 4) can be verified to ensure that the antenna is always tracking the satellite (iPStar-1).

A. SATCOM ANTENNA SYSTEM

A General Dynamic (GD), multiple-size Cassegrain antenna incorporated with precision-formed panels that demonstrates excellent performance in receiving signals. The pedestals are designed with full orbital arc coverage and readily adaptable to ground or rooftop installations. The antenna's electrical

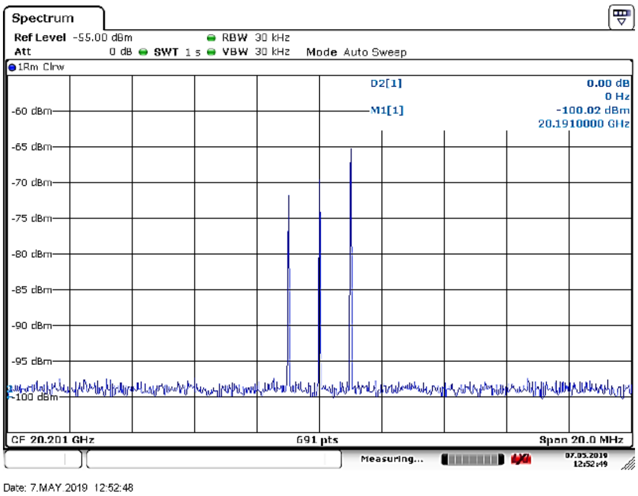

FIGURE 4. Received beacon signal captured from SA.

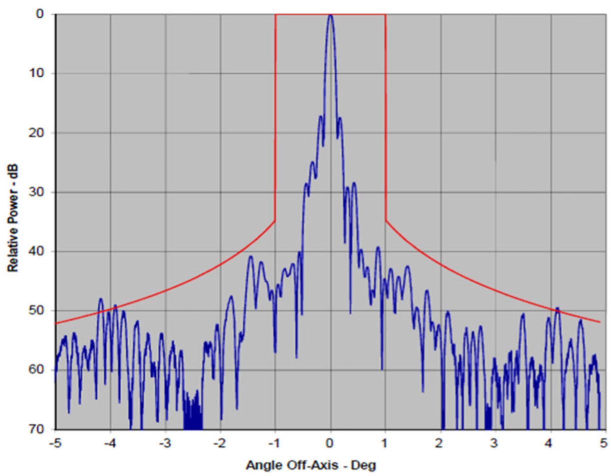

FIGURE 5. Receive pattern cut H-pol +/− 5 Deg, which complies with ITU RS-580.

performance complies with FCC and ITU-RS-580 sidelobe (red line in Figure 5) specifications and Intelsat (F3, E3) and Eutelsat (L, S1) requirements.

The larger the diameter of the antenna such as 13.1m used in this study, the better its radio wavelength is and the more lobes its radiation pattern has [4]. Side lobes in receiving antennas may pick up interfering signals and increase the noise level in the receiver. The side lobe can be minimized by providing a precise panel alignment. Thus, good directional transmission can be achieved.

The selected antenna of 13.1 m provides a receive gain of 63.2 dBi (at 20.2 GHz) that offers a good C/N_{margin} compared with other antennas that are <2.4 m [1]. The added merit of large antenna size could sustain high rainfall conditions and reduce the outage due to high directivity.

With this approach, the main design variable can be determined by comparing the performance of multiple antennas. Such an approach also provides the statistical variation of rainfall to achieve good agreement with observed data.

B. DIGITAL TRACKING RECEIVER SYSTEM (DTR)

DTR (Figure 6) converts the received satellite beacon signals to DC voltage. The voltage is used to control the antenna control unit and uplink power systems. The RF signal, which is L-band, is further analyzed based on the clear sky value that is set as ∼72 dBm (8 Vdc). Each reduction in the input power level is recorded to determine the attenuation level of receiving a beacon signal, as presented in equation (2) [3].

$$\textit{Attenuation}\ (dB) = \textit{Clear Sky level}\,(dBm) - \textit{Received Signal level}\ (dBm) \tag{2}$$

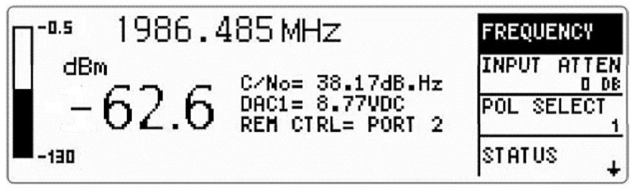

FIGURE 6. DTR typical operational display.

C. ON SITE WEATHER STATION

A Vaisala weather station with a piezoelectric detector sensor located under the weather transmitter is shown in Figure 7. This technology has led to advancements in rain rate collection over the last century. It provides six of the most important weather parameters, namely, air pressure, temperature, humidity, rainfall, wind speed, and wind direction.

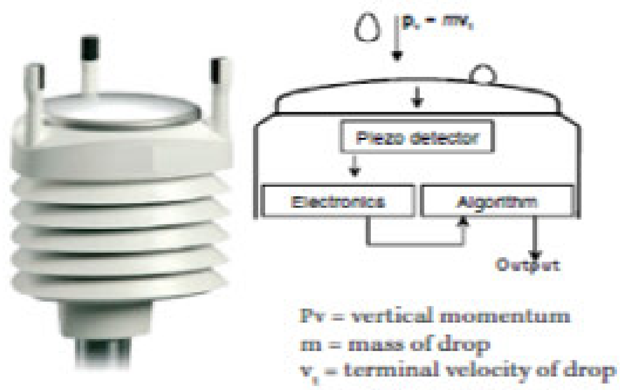

FIGURE 7. Vaisala RAINCAP®sensor technology under the product of weather transmitter WXT536.

The piezoelectric detector is an acoustic sensor used to measure the impact of individual raindrops due to high intensity of rainfall. The intensity output resolution of the sensor is 0.01 mm/h (0.01 in/h), and the intensity observation range is between 0 mm/h and 500 mm/h (0 mm/h and 19.69 in/h). This range provides a good measurement of rain intensity in tropical zones including in the measured area.

TABLE 2. Statistical antenna parameters and availability.

Frequency 20.199827 GHz							
Antenna Size	Gain	C/N (clear sky)	Attenuation (dB)	Total Outage 2017 (hrs)	Total Outage 2018 (hrs)	Availability 2017 (%)	Availability 2018 (%)
0.65 m	22.30 dBi	15 dB	10	12.62	12.98	99.856	99.852
0.85 m	30.00 dBi	17 dB	12	10.69	11.13	99.878	99.873
1.20 m	42.70 dBi	20 dB	14	7.89	9.82	99.910	99.888
7.20 m	56.10 dBi	23 dB	22	2.98	3.51	99.966	99.960
13.10 m	64.30 dBi	29 dB	27	0.53	0.35	99.994	99.996

Thus, specific rain measurement methods show no obvious measurement accuracy advantage, but several unique merits help provide real-time precipitation data [7] Figure 8 shows the recorded rain intensity trend for 2017 in Bukit Jalil.

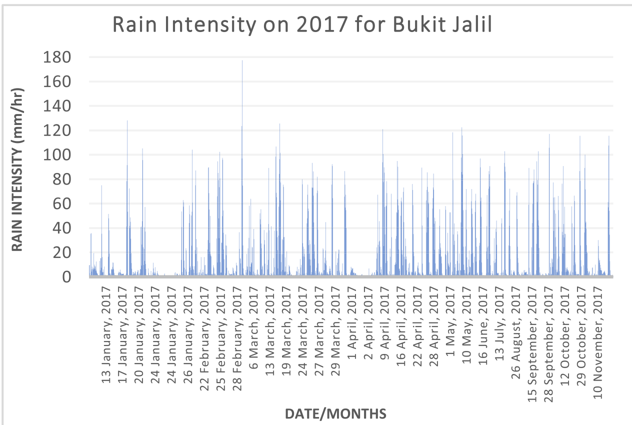

FIGURE 8. Display of rain intensity data recorded from an onsite weather station at Bukit Jalil using a piezoelectric detector.

This presents the role of visual predictive analytics in determining the degree of rain attenuation because the Malaysian meteorological database was unavailable in the analyzed area.

III. METHODOLOGY

Data collection was conducted continuously for two years (2017 to 2018) at two locations, namely, Bukit Jalil (Kuala Lumpur) and Cyberjaya (Selangor), in Malaysia. Multiple antenna types whose sizes ranged from 0.65 m to 13.1 m were compared. The comparison revealed that a large-sized antenna has a high margin and can maintain the downlink signal before a complete outage. This design provides a substantial difference during attenuation calculation and measurement. A statistical analysis of the antenna parameters and its availability is presented in Table 2.

Apart from direct attenuation measurement, rain prediction calculation was performed to determine the attenuation value via the available prediction model. In general, the parameters of ITU-R.P618, DAH, and modified ITU-R are the most commonly used for statistical analysis of rain attenuation prediction. Other evaluation procedures, namely, percentage relative error and root mean square (RMS), was added to the calculation.

Both are recommended by ITU-R P311, with which the error between predicted and measured attenuation was calculated. Mean error μ_v and standard deviation δ_v were used to calculate the RMS value when the preferred prediction method was considered [14].

The measured attenuation varied according to antenna sizes because each antenna provides a different set of specifications. This condition could influence the overall mean error and standard deviation calculation.

Table 3 shows an on-site parameter characterization of Earth–satellite measurement. As recommended, the rain attenuation prediction model for an Earth–satellite link is determined to exceed time percentages in the range of 0.001% to 0.1%. The attenuation on any given path depends on the value of specific attenuation, frequency, polarisation, temperature, path length, and latitude.

TABLE 3. Characteristic of measurement sites.

Measurement Sites		Bukit Jalil	Cyberjaya
Earth Station Location		3.0587∘N 101.6917∘E	2.9348∘N 101.6590∘E
Beacon Frequency		20.199827 GHz (H-pol)	
Satellite		iPStar-1 (119.5∘E)	
Antenna Elevation		68.8 ∘	
Antenna Diameter		13.1m	
Antenna, Hs		8.72m	
Rain Rate 0.001%	2017	177.4 mm/hr	140.2 mm/hr
	2018	194.8 mm/hr	239.8 mm/hr

The beacon signal of the satellite was measured using a spectrum analyzer (Figure 9) and a carrier monitoring system (Figure 10), which continuously logged the data trend. The received beacon signal was then calculated with the measured clear sky signal captured during the maximum beacon reading from DTR. Thus, good analysis of the optimum signal transmission back to Earth is achieved.

The modified ITU-R rain attenuation model is as follows:

$$A_p = A_{0.001}\left(\frac{p}{0.01}\right)^{-(0.3061+0.0524 ln(p)+0.04 ln(A_{0.01})} + \beta(1-p) sin\theta \; dB, \quad (3)$$

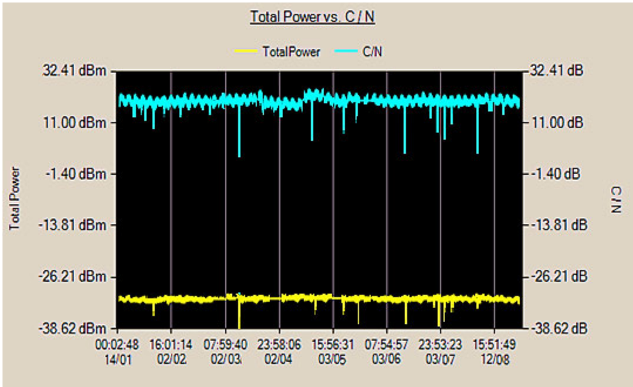

FIGURE 9. Recorded trend of the beacon power level and C/N.

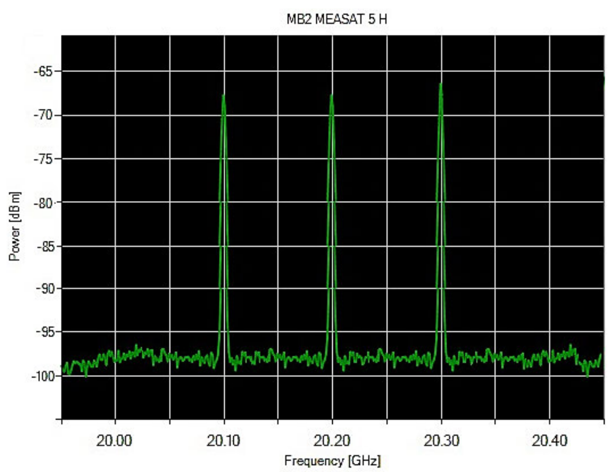

FIGURE 10. Ka-band beacon signal obtained from the carrier monitoring system for the 13.1 m antenna.

where

$$B\begin{cases}0, & if\ p \geq 1\% \\ -0.005\left(|\varphi|-36\right), & if\ p < 1\%.\end{cases}$$

The predicted attenuation from ITU-R 618 is shown below.

$$B = \begin{cases}0, & if\ p \geq 1\%\ or\ |\varphi| \geq 36^{\circ} \\ -0.005\left(|\varphi|-36\right), & if\ p \geq 1\%\ or\ |\varphi| < 36^{\circ}\ and \theta \geq 25^{\circ} \\ -0.005\left(|\varphi|-36\right) \\ \quad +1.8-4.25\sin\theta, & otherwise\end{cases}$$

$$A_p = A_{0.001}\left(\frac{p}{0.01}\right)^{-(0.655+0.33ln(p)+0.045ln(A_{0.01})+\beta(1-p)sin\theta}, dB \quad (4)$$

Simulations using the different rain attenuation models, namely, ITU–R, modified ITU–R and DAH, were further analyzed based on the equation above. The prediction model's calculation was further investigated using the licensed version of Mathworks's MATLAB® software.

IV. MEASUREMENT AND INTERPRETATION

Two years of rainfall data were obtained for analysis, and the time frame was from January 1, 2017 to December 31, 2018. These data were considered for analysis primarily because satellites were made commercially available to broadcasters starting from 2017 onwards under the Ka-band frequency. The receiving beacon signal and rain rate data were logged every second to ensure that there is no missing data for analysis.

A comparison of five receivers was conducted based on the measured data, and the results showed that the 13.1 m antenna provides good measurement and signal margin results. The attenuation reading is presented in Figures 11 to 14.

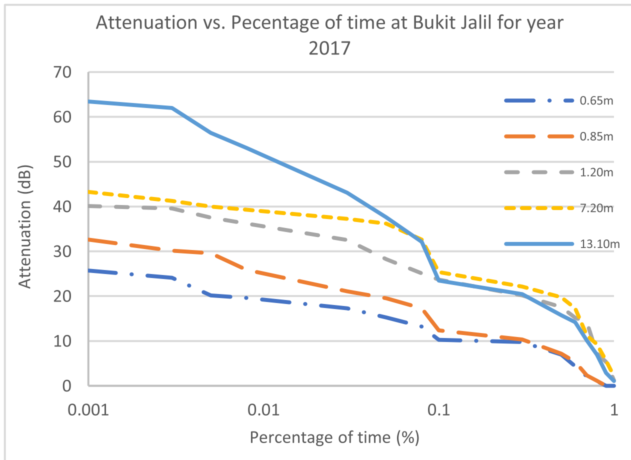

FIGURE 11. Comparison of the beacon attenuation signals of five antenna sizes for 2017 at Bukit Jalil.

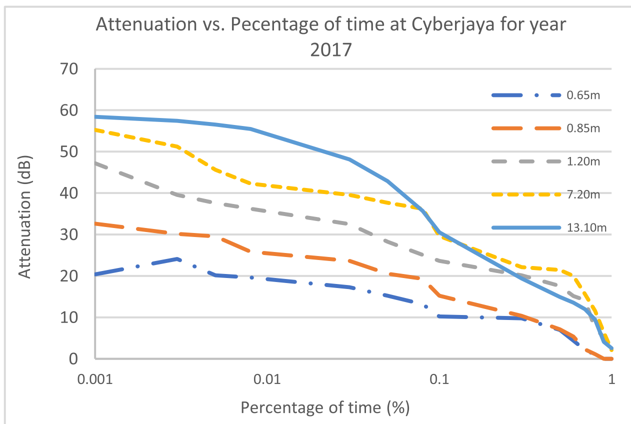

FIGURE 12. Comparison of the beacon attenuation signals of five antenna sizes for 2017 at Cyberjaya.

The statistical measurement results were summarised in Table 4 to 7, together with the analyzed prediction model. The data for the 13.1 m antenna were examined for further recommendations.

V. RESULT AND DISCUSSION

The experimental results indicated that the measured $R_{0.01}$ rainfall rate at Bukit Jalil was 177.4 and 140.2 mm/hr for 2017 and 2018, respectively. For Cyberjaya, the rainfall rate

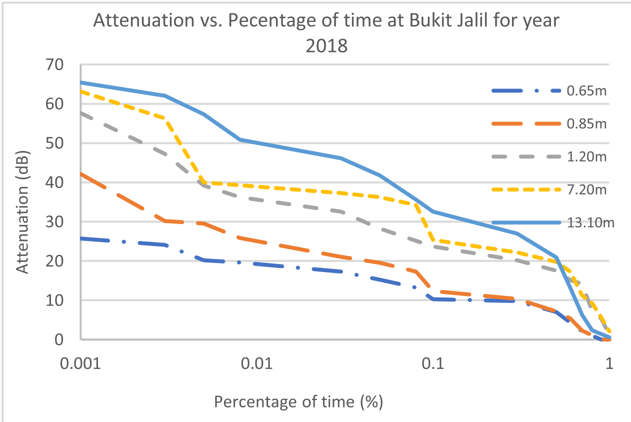

FIGURE 13. Comparison of the beacon attenuation signals of five antenna sizes for 2018 at Bukit Jalil.

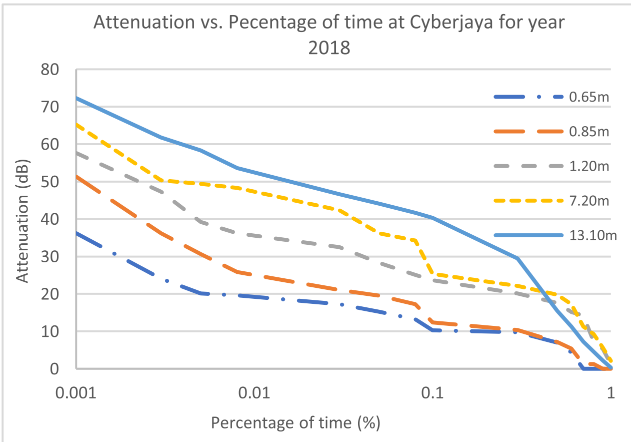

FIGURE 14. Comparison of the beacon attenuation signals of five antenna sizes for 2018 at Cyberjaya.

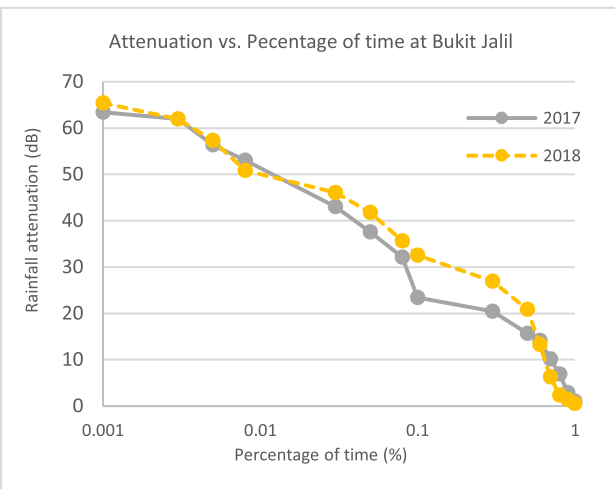

FIGURE 15. Measured rain attenuation for the duration of two years at Bukit Jalil.

was 194.8 and 239.8 mm/hr for 2017 and 2018, respectively. The annual cumulative distribution of rain attenuation based at both locations are presented in Figures 15 and 16.

TABLE 4. Statistical analysis of the predicted model and the measured data for 2017 at Bukit Jalil.

	2017				
	X	ITU-R	DAH	ITU-R (M)	Measured
Bukit Jalil	0.001	55.68	62.27	62.42	63.42
	0.003	47.56	54.41	50.85	61.98
	0.005	44.51	49.62	46.27	56.41
	0.008	41.23	46.64	44.05	53.04
	0.03	30.56	36.05	34.02	43.05
	0.05	26.24	31.19	29.06	37.62
	0.08	22.31	25.7	23.25	32.10
	0.1	20.48	23.07	20.7	23.46
	0.3	11.89	10.46	10.31	20.43
	0.5	8.23	7.23	7.95	15.71
	0.6	7.00	6.15	6.62	14.19
	0.7	6.01	5.28	5.11	10.14
	0.8	5.19	4.56	4.31	6.94
	0.9	4.51	3.96	3.23	2.89
	1	3.93	3.45	2.35	1.07

TABLE 5. Statistical analysis of the predicted model and the measured data for 2017 at Bukit Jalil.

	2017				
	X	ITU-R	DAH	ITU-R (M)	Measured
Cyberjaya	0.001	33.421	38.092	43.27	58.42
	0.003	30.635	35.169	40.07	57.46
	0.005	28.629	32.976	37.24	56.54
	0.008	26.486	30.603	31.88	55.51
	0.03	19.587	22.828	18.28	48.16
	0.05	16.807	19.655	14.12	42.87
	0.08	14.281	16.752	10.94	35.71
	0.1	13.102	15.391	9.65	30.57
	0.3	7.563	8.949	5.21	19.38
	0.5	5.199	6.172	4.11	14.94
	0.6	4.408	5.24	3.85	13.57
	0.7	3.769	4.485	3.69	11.99
	0.8	3.243	3.862	3.60	9.48
	0.9	2.803	3.341	3.56	4.06
	1	2.431	2.899	3.56	2.56

The aim is to confirm which model is preferred for selection. As shown in Figure 15 and 16, the maximum attenuation values recorded in Bukit Jalil for 0.001% of the time were 63.42 and 65.40 dB for 2017 and 2018, respectively. Meanwhile for Cyberjaya, the recorded attenuation values were 58.4 and 72.29 dB for 2017 and 2018, respectively.

TABLE 6. Statistical analysis of the predicted model and the measured data for 2018 at Bukit Jalil.

	2017				
	X	ITU-R	DAH	ITU-R (M)	Measured
Cyberjaya	0.001	33.421	38.092	43.27	58.42
	0.003	30.635	35.169	40.07	57.46
	0.005	28.629	32.976	37.24	56.54
	0.008	26.486	30.603	31.88	55.51
	0.03	19.587	22.828	18.28	48.16
	0.05	16.807	19.655	14.12	42.87
	0.08	14.281	16.752	10.94	35.71
	0.1	13.102	15.391	9.65	30.57
	0.3	7.563	8.949	5.21	19.38
	0.5	5.199	6.172	4.11	14.94
	0.6	4.408	5.24	3.85	13.57
	0.7	3.769	4.485	3.69	11.99
	0.8	3.243	3.862	3.60	9.48
	0.9	2.803	3.341	3.56	4.06
	1	2.431	2.899	3.56	2.56

TABLE 7. Statistical analysis of the predicted model and the measured data for 2018 at Cyberjaya.

	2018				
	X	ITU-R	DAH	ITU-R (M)	Measured
Cyberjaya	0.001	61.59	70.15	77.65	72.29
	0.003	56.97	61.83	62.96	61.80
	0.005	53.43	57.57	54.68	58.31
	0.008	49.57	55.04	46.87	53.62
	0.03	36.89	46.47	26.93	46.60
	0.05	31.72	41.77	20.80	44.12
	0.08	27.00	37.48	16.10	41.64
	0.1	24.79	34.48	14.20	40.33
	0.3	14.40	21.06	7.60	29.45
	0.5	9.97	11.04	5.94	15.50
	0.6	8.48	8.70	5.55	11.28
	0.7	7.28	6.61	5.30	7.27
	0.8	6.29	5.71	5.14	4.52
	0.9	5.46	4.95	5.06	2.21
	1	4.75	4.32	5.04	0.31

A comparison of the analysis and measured data is presented in Figures 17 to 20. The measured rain attenuation model was not immediately close to the available ITU-R, modified ITU-R or DAH model. This result could be due to the underestimation of pattern changes in tropical climates. However, the modified ITU-R rain attenuation model visually

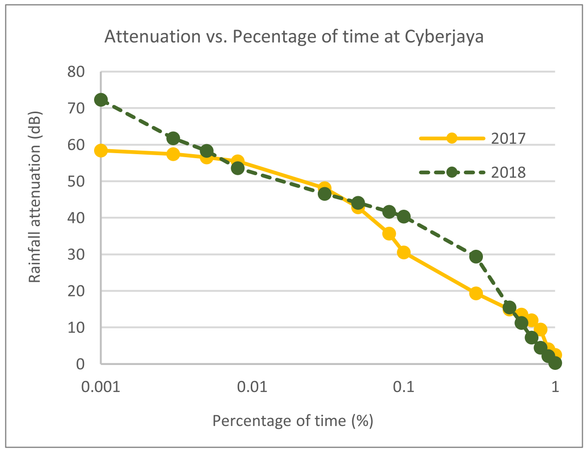

FIGURE 16. Measured rain attenuation for the duration of two years at Cyberjaya.

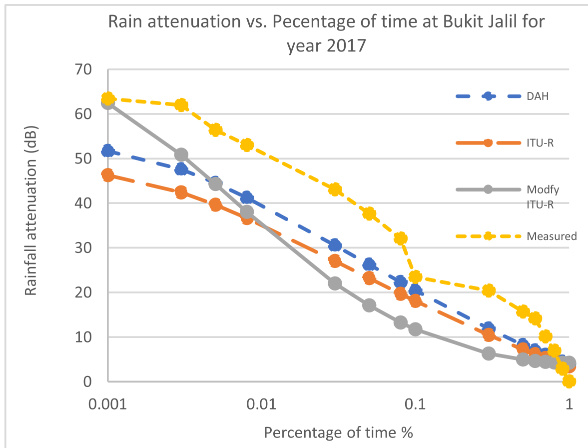

FIGURE 17. Comparison of measured rain attenuation using an available model for Bukit Jalil in 2017.

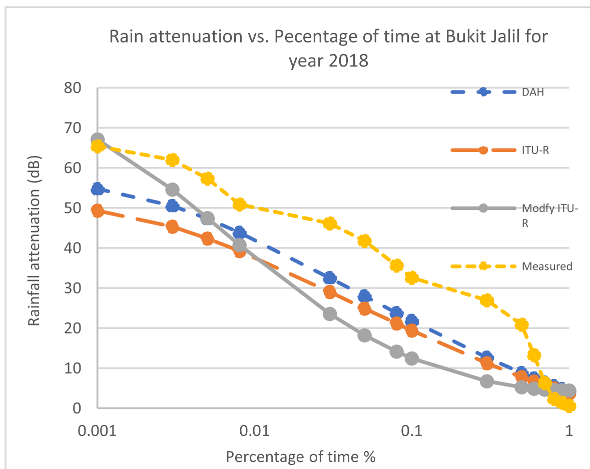

FIGURE 18. Comparison of measured rain attenuation using an available model for Bukit Jalil in 2018.

fit the measured data. The accuracy of the model data was further calculated using the percentage error because visual approximation is not the recommended means of determining the best prediction method.

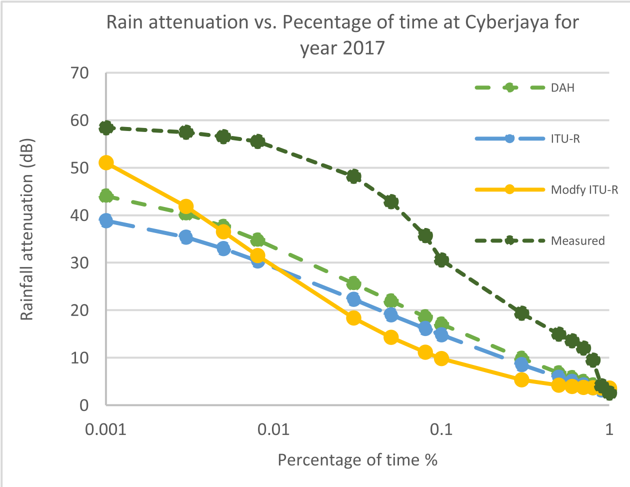

FIGURE 19. Comparison of measured rain attenuation using an available model for Cyberjaya in 2017.

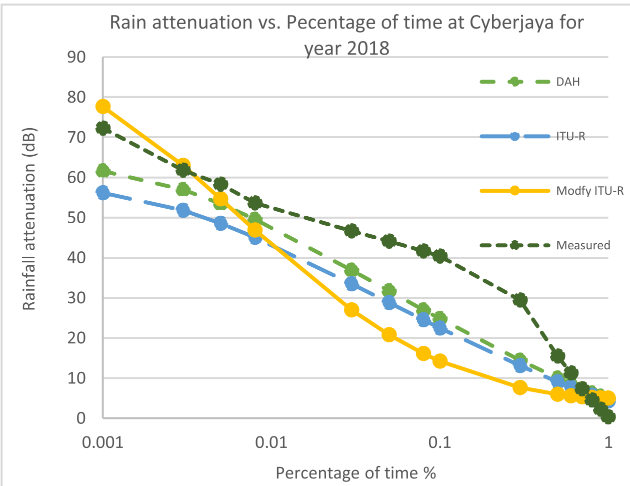

FIGURE 20. Comparison of measured rain attenuation using an available model for Cyberjaya in 2018.

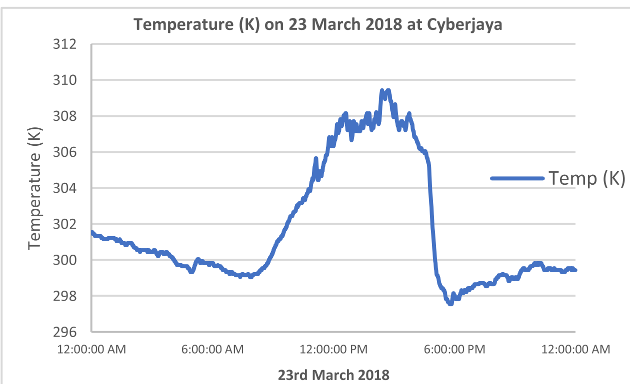

FIGURE 21. Observed temperature changes on March 23, 2018 at Cyberjaya.

Tables 9 to 12 list the mean ($\mu_{\mathbf{v}}$), standard deviation ($\delta_{\mathbf{v}}$) and RMS (%) values for both years and locations. Research evidence indicated that the most optimum prediction model is the model with the lowest RMS value or whose value approximates zero [23]. However, this is impossible to achieve based on the predicted measured value. A possible reason could be the impact of the coefficient, frozen & liquid precipitation and rain height. The earth-space path also contributes to the available prediction model or the factor of additional attenuation, which might affect the gain over temperature (G/T) of the measured value, as indicated in Figure 21.

The LNA temperature calculated using (equation 5), in the antenna hub highly dependent on the changes in G/T [24].

TABLE 8. G/T (dB) measurement at a different time interval based on captured temperature.

Parameter \Time	Freq (GHz)	EL Angle	T LNA (K)	T Load (K)	Y factor (dB)
T1	20.2	68.8	66.32	306	3.96
T2	20.2	68.8	59.9	297	3.44
T3	20.2	68.8	64.78	288	4.23
T4	20.2	68.8	64.78	309	4.33
	Y factor NUM	Tsys (K)	Tsys (dB)	RX Ant Gain (dBi)	G/T (dB)
T1	2.49	149.59	21.75	56.2	40.72
T2	2.21	165.72	22.19	56.2	40.29
T3	2.65	140.00	21.46	56.2	41.01
T4	2.71	147.76	21.39	56.2	45.63

TABLE 9. Statistical analysis of the mean, standard deviation, and RMS error between predicted and measured data for Bukit Jalil for 2017.

Bukit Jalil for 2017			
	DAH	ITU-R	Modify ITU-R
Mean, μ_v	-21.91	-19.70	-23.57
Std Dev, δ_v	25.78	19.34	21.34
RMS, (%)	33.83	27.61	31.80

TABLE 10. Statistical analysis of the mean, standard deviation, and RMS error between predicted and measured data for Bukit Jalil for 2018.

Bukit Jalil for 2018			
	DAH	ITU-R	Modify ITU-R
Mean, μ_v	-19.95	-13.49	-22.02
Std Dev, δ_v	24.05	23.14	30.71
RMS, (%)	31.25	26.79	37.79

TABLE 11. Statistical analysis of the mean, standard deviation, and RMS error between predicted and measured data for Cyberjaya for 2017.

Cyberjaya for 2017			
	DAH	ITU-R	Modify ITU-R
Mean, μ_v	-4.81	-27.28	-19.96
Std Dev, δ_v	47.71	21.34	27.61
RMS, (%)	47.95	34.46	34.07

TABLE 12. Statistical analysis of the mean, standard deviation, and RMS error between predicted and measured data for Cyberjaya for 2018.

Cyberjaya for 2018			
	DAH	ITU-R	Modify ITU-R
Mean, μ_v	16.32	-6.19	-11.84
Std Dev, δ_v	19.75	12.97	17.96
RMS, (%)	25.62	14.37	21.51

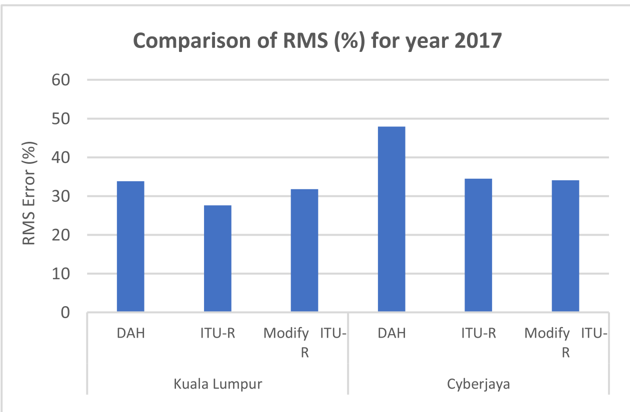

FIGURE 22. Compared mean error of the two sites' attenuation in comparison with the prediction model for 2017.

Each hub varies in terms of temperature and provides a different reading of antenna gain and different C/Nmargin values of the received beacon signal.

In Malaysia, isotherm height changes with humidity [5]. In other words, isotherm height reduces with any increases to the relative ground humidity [25]. The comparison between the real data (measured) and predictions made by the ITU-R Modify-R and DAH models is shown in Figures 22 and 23.

$$Tsys\,(K) = \frac{T_{lna}\,(K) + T_{load}(K)}{Y\ factor\ NUM} \quad (5)$$

$Y\ actor\ NUM = 10^x\ (Y\ factor\ dB\ /10),$
$Tsys\ dB = 10\ \log\ Tsys\ Kelvin,$
$G/T\ dBk = Rx\ Ant\ Gain\ -\ Tsys\ dB$
$T\ Load\ (K) = Ambient\ Hub\ Temp\ in\ oC + 273$

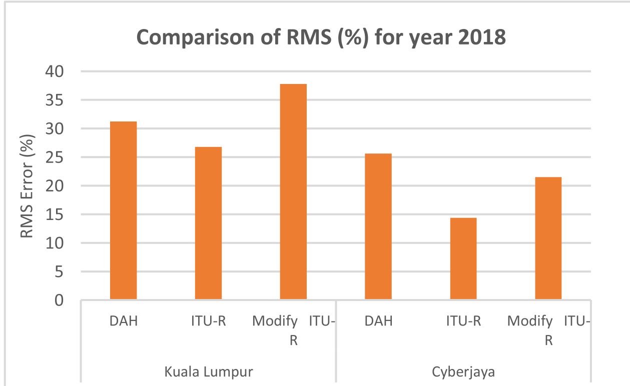

FIGURE 23. Compared mean error for the two sites' attenuation in comparison with the prediction model for 2018.

VI. CONCLUSION

Amongst all prediction models available at present, ITU-R still has the lowest RMS value, but not as near as zero, as revealed by the comparison with other recommended models. However, the effect of rain cannot be predicted nor expected due to possible shifts in rain patterns in tropical regions, particularly Malaysia where ITU-R modelled still require further improvement. This situation requires further investigation of existing models, and long-term measured data are necessary for precise analyses. The usage of larger diameter antennas for prediction of rain intensity provides a wider range of signals data that is received, thus increases the efficiency of the results. The application of the Ka-band is new to Malaysia, but such an application ensures a reliable prediction in cases where extensive broader data are required. With a precise measurement value from an antenna with a diameter of above 7.2m, it would provide results depicting the best percentage error and would be recommended for the future researcher.

REFERENCES

[1] S. L. Jong, H. Y. Lam, M. D'Amico, and J. Din, "Analysis of precipitation characteristics over Southern Peninsular Malaysia for satellite propagation application," in *Proc. URSI Asia–Pacific Radio Sci. Conf. (URSI AP-RASC)*, Aug. 2016, pp. 1729–1732.

[2] S. Shrestha and D.-Y. Choi, "Diurnal and monthly variations of rain rate and rain attenuation on Ka-band satellite communication in South Korea," *Prog. Electromagn. Res.*, vol. 80, pp. 151–171, 2018.

[3] S. Shrestha, I. Nadeem, J. Ghimire, S.-W. Kim, H. G. Yu, and D.-Y. Choi, "Seasonal and diurnal variations of rain attenuation measured with the Koreasat 6 at 20.73 GHz," in *Proc. Int. Conf. Inf. Commun. Technol. Converg. (ICTC)*, Oct. 2017.

[4] R. Xue, H. Yu, and Q. Cheng, "Adaptive coded modulation based on continuous phase modulation for inter-satellite links of global navigation satellite systems," *IEEE Access*, vol. 6, pp. 20652–20662, 2018.

[5] J. S. Mandeep, O. W. Hui, M. Abdullah, M. Tariqul, M. Ismail, W. Suparta, B. Yatim, P. S. Menon, and H. Abdullah, "Modified ITU-R rain attenuation model for equatorial climate," in *Proc. IEEE IconSpace*, Penang, Malaysia, Jul. 2011.

[6] M. Ahmed, M. Sultan, E. Yan, and J. Wahr, "Assessing and improving land surface model outputs over Africa using GRACE, field, and remote sensing data," *Surv. Geophys.*, vol. 37, pp. 529–556, Feb. 2016.

[7] V. Ramachandran and V. Kumar, "Modified rain attenuation model for tropical regions for Ku-band signals," *Int. J. Satell. Commun. Netw.*, vol. 25, pp. 53–67, Jan. 2006, doi: 10.1002/sat.846.

[8] M. S. J. Singh, S. I. S. Hassan, M. F. Ain, F. Ghani, K. Igarashi, K. Tanaka, and M. Iida, "Rain attenuation model for South East Asia countries," *Electron. Lett.*, vol. 43, pp. 75–77, Jan. 2007, doi: 10.1049/el:20072677.

[9] R. Singh and R. Acharya, "Development of a new global model for estimating one-minute rainfall rate," *IEEE Trans. Geosci. Remote Sens.*, vol. 56, no. 11, pp. 6462–6468, Nov. 2018.

[10] *Rain Height Model for Prediction Methods*, document Rec. ITU-R P.839-4, International Telecommunication Union, Geneva, Switzerland, 2001.

[11] W. L. Stutzman and W. K. Dishman, "A simple model for the estimation of rain-induced attenuation along Earth-space paths at millimeter wavelengths," *Radio Sci.*, vol. 17, no. 6, pp. 1465–1476, 1982.

[12] Z. X. Zhou, L. W. Li, T. S. Yeo, and M. S. Leong, "Cumulative distributions of rainfall rate and microwave attenuation in Singapore's tropical region," *Radio Sci.*, vol. 35, no. 3, pp. 751–756, 2000, doi: 10.1029/1999RS900094.

[13] V. Kumar and V. Ramachandran, "Rain-attenuation measurement at 11.6 GHz in Suva, Fiji," *Electron. Lett.*, vol. 40, no. 22, pp. 1429–1431, 2004.

[14] S. Shrestha and D.-Y. Choi, "Characterization of rain specific attenuation and frequency scaling method for satellite communication in South Korea," *Int. J. Antennas Propag.*, vol. 2017, pp. 1–16, 2017.

[15] A. M. Al-Saegh, A. Sali, J. S. Mandeep, A. Ismail, H. J. A. Al-Jumaily, and C. Gomes, "Atmospheric propagation model for satellitecommunications," in *MATLAB Applications for the Practical Engineer*. Rijeka, Croatia: InTech, 2014, ch. 9, doi: 10.5772/58238.

[16] P. Setiyanto, "Prediction models of rain rate (RO.01) and rain attenuation in ku-band satellite communications system for Indonesian archipelago," M.S. thesis, Dept. Elect. Eng., Inst. Teknologi Bandung, Bandung, Indonesia, 2003.

[17] J. Suryana, U. Sastrokusumo, H. Wundarto, K. Igarashi, and H. Minakoshi, "Study on wet antenna at Ku-band for further considerations of propagation measurement and antenna design," in *Proc. Asia–Pasific Radio Sci. Conf.*, Tokyo, Japan, 2001.

[18] R. K. Crane, "Prediction of attenuation by rain," *IEEE Trans. Commun.*, vol. COM-28, no. 9, pp. 1717–1733, Sep. 1980, doi: 10.1109/TCOM.1980.1094844.

[19] *Rain Height Model for Prediction Methods*, document Rec. ITU-R P.618-13, International Telecommunication Union, Geneva, Switzerland, 2001.

[20] *Rain Height Model for Prediction Methods*, document Rec. ITU-R P.311-17, International Telecommunication Union, Geneva, Switzerland, 2001.

[21] H. Fang, H. K. Beaudoing, M. Rodell, W. L. Teng, and B. E. Vollmer, "Global land data assimilation system (GLDAS) products, services and application from NASA hydrology data and information services center (HDISC)," in *Proc. ASPRS Annu. Conf.*, Baltimore, MD, USA, Mar. 2009, pp. 151-1–151-9.

[22] A. Dissanayake, J. Allnutt, and F. Haidara, "A prediction model that combines rain attenuation and other propagation impairments along earth-satellite paths," *IEEE Trans. Antennas Propag.*, vol. 45, no. 10, pp. 1546–1558, Oct. 1997.

[23] N. Perez Garcia and L. Da Silva Mello, "Improved method for prediction of rain attenuation in terrestrial links," *Electron. Lett.*, vol. 40, no. 11, pp. 847–848, 2004.

[24] J. S. Mandeep, R. Nalinggam, and W. B. Ismail, "Cumulative distribution of rainfall data for tropical countries," *J. Sci. Res. Essays*, vol. 6, no. 2, pp. 447–452, 2011.

[25] A. H. Al-Jumaily, A. Sali, A. Ismail, J. Mandeep, and A. M. Al-Saegh, "Performance analysis of rain attenuation at Ku-band in Malaysia," in *Proc. IEEE IconSpace*, Malacca, Malaysia, Jul. 2013, pp. 1–3.

[26] L. S. Chuan, S. Ru-Tian, and Y. P. Hon, "Ka band satellite communications design analysis and optimization," in *Proc. DSTA HORIZONS*, 2015.

[27] K. Chakravarty and A. Maitra, "Rain attenuation studies over an earth–space path at a tropical location," *J. Atmos. Sol.-Terr. Phys.*, vol. 72, no. 1, pp. 135–138, Jan. 2010.

[28] J. Mandeep, "Rain attenuation statistics over a terrestrial link at 32.6 GHz at Malaysia," *IET Microw., Antennas Propag.*, vol. 3, no. 7, pp. 1086–1093, 2009.

[29] A. M. Al-Saegh, "Atmospheric impairments on satellite signal in the middle-east: Characterization and analysis," *J. Aeronaut. Aerosp. Eng.*, vol. 6, p. 2, 2017, doi: 10.4172/2168-9792-C1-017.

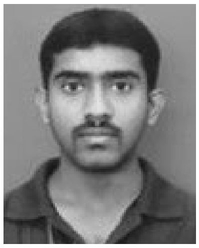

P. M. KALAIVAANAN (Student Member, IEEE) received the B.Eng. degree in communication engineering from University Malaysia Perlis, in 2007, and the master's degree in engineering management from University Putra Malaysia, in 2016, where he is currently pursuing the Ph.D. degree in communication and network engineering. He is a Postdoctoral Researcher with the Faculty of Engineering, University Putra Malaysia (UPM). His main research interests include satellite communication and visible light communication (VLC).

ADUWATI SALI (Senior Member, IEEE) received the Ph.D. degree in mobile and satellite communications from the University of Surrey, U.K., in July 2009, the M.Sc. degree in communications and network engineering from UPM, Malaysia, in April 2002, and the B.Eng. degree in electrical electronics engineering (communications) from the University of Edinburgh, U.K., in 1999. She worked as an Assistant Manager at Telekom Malaysia Bhd., from 1999 to 2000. She has been a Professor with the Department of Computer and Communication Systems, Faculty of Engineering, Universiti Putra Malaysia (UPM), since December 2013. She is a Deputy Director of the UPM Research Management Centre (RMC) and is responsible for research planning and knowledge management. She is also a Chartered Engineer (C.Eng.) registered under the UK Engineering Council and a Professional Engineer (P.Eng.) under the Board of Engineers Malaysia (BEM). Her research interests include radio resource management, MAC layer protocols, satellite communications, satellite-assisted emergency communications, the IoT systems for environmental monitoring, and 3D video transmission over wireless networks. She was also a recipient of the 2018 Top Research Scientists Malaysia (TRSM) Award from the Academy of Sciences Malaysia (ASM). She is involved with the IEEE as a chairperson to ComSoc/VTS Malaysia, in 2017 and 2018, and Young Professionals (YP), in 2015, Young Scientists Network-Academy of Sciences Malaysia (YSN-ASM) as the Chair, in 2018, and the Co-Chair, in 2017, for Science Policy. She was involved with EU-IST Satellite Network of Excellence (SatNEx) I and II, from 2004 to 2009. She is the Principal Investigator and Collaborator in projects under local and international funding bodies, namely, Malaysian Ministry of Science, Technology and Innovation (MOSTI), Malaysian Ministry of Higher Education (MoHE), Malaysian Communications and Multimedia Commission (MCMC), Research University Grant Scheme (RUGS) (now known as Putra Initiative Grant) UPM, the Academy of Sciences for the Developing World (TWAS-COMSTECH) Joint Grants, EU Horizon 2020 Research and Innovation Staff Exchange (H2020-RISE), and NICT Japa–ASEAN IVO. She provided consultation to the Malaysian Ministry of Information and Multimedia, Malaysian Ministry of Higher Education, National Space Agency (ANGKASA), ATSB Bhd., and Petronas Bhd. on projects related to mobile and satellite communications. In 2014, due to the fateful disappearance of MH370, she appeared in printed and broadcasting media, specifically Astro Awani, RTM, TV Al-Hijrah, BERNAMA, Harian Metro, and Metro Ahad, regarding the analysis of satellite communication in tracking the missing aircraft.

RAJA SYAMSUL AZMIR RAJA ABDULLAH (Senior Member, IEEE) received the B.Eng. degree in electronic and electrical engineering, the M.Sc. degree in communication system engineering, and the Ph.D. degree in radar and microwave system from the University of Birmingham, U.K., in 2000, 2001, and 2005, respectively. His researches focus on microwave systems, radar systems, and wireless sensor networks, and he has been involved in the development of hardware and software for radar sensors and wireless sensor networks (WSNs). He has contributed to the development of the advanced practical forward scattering radar (FSR) system; the system has been adopted for various applications, including civil, military, and medical. With the addition of an intelligent system, the advanced FSR system can automatically detect and classify most ground and air targets. Recent development focuses on the high-resolution radar network (RSN), which can be applied to small-object detection and classification. By adopting WSN advantages, the drawbacks of traditional radar can be compensated. Future radar will have the size of a computer mouse compared with the huge radar set mounted on towers at present.

SYAMSURI YAAKOB (Senior Member, IEEE) received the B.Eng. and M.Eng.Sc. degrees in electronic engineering from Kin's College London and Multimedia University (MMU), Cyberjaya, in 1998 and 2010, respectively, and the Ph.D. degree in millimeter-wave radio over fiber system from Universiti Teknologi Malaysia (UTM), in 2014. He was a Satellite Engineer with Telekom Malaysia, in 1998, and a Senior Researcher with TM Research and Development Sdn. Bhd. (TMR&D), in 2004. He is currently an Associate Professor with the Department of Computer and Communication Systems Engineering, Faculty of Engineering, Universiti Putra Malaysia (UPM). His current research interests include millimeter-wave radio over fiber systems, passive optical networks, optical communication systems, and access network technologies.

MANDEEP JIT SINGH (Senior Member, IEEE) was born in Malaysia, in 1975. He is currently a Professor with the Department of Electrical, Electronic and Systems Engineering, Universiti Kebangsaan Malaysia (UKM), and a Visiting Professor with Covenant University, Nigeria. He is also the Advisor of the Engineering Education Technical Division (E2TD), Institute of Engineers, Malaysia. He is the author or coauthor of more than 240 research articles in antenna and microwave RF. He was also a recipient of more than 40 research grants (national and international). Thus far, his publications have been cited 959 times, and his H-index is 15. His research interests include communication antenna design, radiowave propagation, satellite antennas, and the IOT. He received several international and national medal awards for his research and innovation. He currently serves as the Editor-in-Chief for *Greener Journal of Electronics and the Communication* and an Associate Editor for *Journal of Electrical and Computer Engineering*, Hindawi.

ALI M. AL-SAEGH (Member, IEEE) was born in Baghdad, Iraq, in April 1984. He received the B.Sc. degree in electronic and communications engineering from Nahrain University, Iraq, in 2005, the M.Sc. degree in satellite engineering from the Electronic and Communications Engineering Department, Nahrain University, in 2008, and the Ph.D. degree in wireless communications engineering from the Computer and Communication System Engineering Department, Universiti Putra Malaysia (UPM), Selangor, Malaysia, in 2015. From 2009 to 2012, he served as a Lecturer with the Computer Engineering Techniques and Communications Engineering Departments, Al-Mamoun University College, Iraq. From 2012 to 2013, he worked as a Research Assistant with the Department of Computer and Communication Systems Engineering, UPM. Since 2015, he has been a Senior Lecturer with the Computer Engineering Techniques Department, Al-Mamoun University College. His areas of specialization are radiowave propagation, satellite communications, atmospheric impairment prediction, channel modeling, multimedia transmission, and resource management. He is a member of several groups and associations, including the satellite communications group in UPM, Iraqi engineering and academic associations, and several IEEE societies and communities.